Part IV

Soft Ground

Consolidation Analysis

Chapter 1 Finite Element Analysis

Chapter 2 1-Dimension Theoretical Analsys

Soft Ground

Consolidation Analysis / 001

Chapter 1 **Finite Element Analysis / 002**

1.1 Governing Equations / 002
1.2 Finite Element Formulation / 004
1.3 Properties of Consolidation Elements / 009
1.3.1 Degrees of Freedom for Plane Strain Elements / 010
1.4 Cautionary Points for Consolidation Analysis / 012
1.4.1 Time and Loading Input / 012

Chapter 2 **1-Dimensional Theoretical Analysis / 014**

2.1 Introduction / 014
2.2 Settlement Calculation Methods / 015
2.2.1 Consolidation Settlement of Cohesive Soil / 015
2.2.2 Settlement of Sandy Soil / 018
2.2.3 Rebound of Cohesive Soil / 020
2.2.4 Secondary Consolidation Settlement / 022
2.3 Calculation of the Effective Overburden Pressure and the Increase in Vertical Stress / 024
2.3.1 Effective Overburden Pressure / 024
2.3.2 Embankment Load / 024
2.3.3 Point Load / 026
2.3.4 Line Load / 026
2.3.5 Strip Load / 027

2.3.6 Rectangular Load / 028
2.3.7 Calculation of Increase in Ground Stress / 029
2.3.8 Loading Distance of Embankment Load / 030
2.4 Calculation of the Degree of Consolidation Relative to Settlement Time / 032
2.4.1 Consolidation Time for Unimproved Soil / 032
2.4.2 Conversion of the Thickness of Consolidation Layer / 032
2.4.3 Calculation of the Degree of Consolidation by Different Drainage Methods / 035
2.5 Increase in Ground Strength due to Embankment Load / 049
2.5.1 General Equation / 049
2.5.2 Strength Increase due to SCP or GCP Process / 049
2.6 Settlement over Time under Staged Loading / 051
2.6.1 Introduction / 051
2.6.2 Total Load Method / 051
2.6.3 Individual Load Method / 058

Consolidation Analysis

Consolidation analysis is associated with drained/undrained analysis where the process of dissipation of excess pore water pressure is calculated. The excess pore water pressure takes place when the water resists loadings.

The entrapped water, which has the ability to resist loading, slowly drains over time by applying drainage boundary conditions. The excess pore water pressure thus dissipates, which results in the transfer of internal force to the soil skeleton leading to the deformation of the soil skeleton. The decrease in water pressure results in the increase in the effective pressure, which exists in the soil skeleton.

Consolidation analysis addresses the reduction in excess pore water pressure resulting in the increase in effective pressure with respect to time. During the process, the deformation of the soil skeleton is induced and accumulated over time exhibiting the behavior of ground soil settlement in the direction of gravity.

The increasing deformation with respect to time induces settlement in foundations of a structure. The differential settlement of the foundations has a great influence on the structural stability.

In consolidation analysis, ground failure is less likely to occur since the density, stiffness and strength of the ground soil increase with time. Undrained analysis generally precedes in consolidation analysis. If failure does not occur in the undrained analysis, failure does not occur in consolidation analysis.

Consolidation analysis is largely classified into theoretical one-dimensional consolidation analysis method and the finite element method. One-dimensional consolidation analysis enables the user to readily obtain the results through a simple process, but it is limited to two-dimensional analysis and is restricted in many aspects in a generalized ground analysis of complex geometry. The finite element analysis method is not so restricted in a generalized or complex ground analysis, but the modeling and analysis may take a long time. SoilWorks supports both analysis methods.

Chapter 1

Finite Element Analysis

1.1 Governing Equations

Up until now, solid and fluid analyses have been considered individually or by superposition. However, Biot has formulated the theory of coupled solid-fluid interaction applied to soil mechanics. Ground is treated as porous elastic solid, and the fluid in the pores is coupled with the solid based on the conditions of compressibility and continuity.

The governing equation of Biot is given in Eq. (1.1.1).

$$\frac{K}{\gamma_w}\left[k_x\frac{\partial^2 p_w}{\partial x^2}+k_y\frac{\partial^2 p_w}{\partial y^2}+k_z\frac{\partial^2 p_w}{\partial z^2}\right]=\frac{\partial p_w}{\partial t}-\frac{\partial p}{\partial t} \tag{1.1.1}$$

where,

K : Bulk modulus of ground

p : Average total stress

A two dimensional state is assumed to simplify the equation. When no element load exists in an equilibrium condition, the rate of change in effective stress is increased by the rate of change in pore water pressure as in Eq. (1.1.2).

$$\begin{aligned}\frac{\partial \sigma'_x}{\partial x}+\frac{\partial \tau_{xy}}{\partial y}+\frac{\partial p_w}{\partial x}=0\\ \frac{\partial \tau_{xy}}{\partial x}+\frac{\partial \sigma'_y}{\partial y}+\frac{\partial p_w}{\partial y}=0\end{aligned} \tag{1.1.2}$$

The constitutive rules for solid Eq. (1.1.1) and fluid Eq. (1.1.2) have been separately defined before. If full saturation and incompressibility are finally assumed, the discharge of water from the ground elements reduces the volume of the elements. Accordingly the next equation is expressed.

$$\frac{\partial q_x}{\partial x}+\frac{\partial q_y}{\partial y}=-\frac{d}{dt}\left(\frac{\partial u}{\partial x}+\frac{\partial v}{\partial y}\right) \tag{1.1.3}$$

The third differential equation from Eq. (1.1.1) is given as Eq. (1.1.4).

$$\frac{k_x}{\gamma_w}\frac{\partial^2 p_w}{\partial x^2}+\frac{k_y}{\gamma_w}\frac{\partial^2 p_w}{\partial y^2}+\frac{d}{dt}\left(\frac{\partial u}{\partial x}+\frac{\partial v}{\partial y}\right)=0 \tag{1.1.4}$$

1.2 Finite Element Formulation

In order to analyze physical and flow coupled problems taking place in the ground, two equilibrium conditions of the physical problem and the groundwater flow must be satisfied. For this, the condition of energy equilibrium of the physical problem developing in the soil particles is first derived using the principle of virtual work.

The internal virtual work of saturated soil, W_{in} can be derived as follows:

$$W_{in} = \int_V \delta \boldsymbol{\varepsilon}^T \, \Delta \boldsymbol{\sigma} \, dV \tag{1.2.1}$$

where, the total stress, $\boldsymbol{\sigma}$ can be defined by,

$$\boldsymbol{\sigma} = \boldsymbol{\sigma}' \mathbf{m} \sigma_w = \begin{Bmatrix} \sigma'_{xx} \\ \sigma'_{yy} \\ \sigma'_{zz} \\ \tau_{xy} \\ \tau_{yz} \\ \tau_{zx} \end{Bmatrix} + \begin{Bmatrix} 1 \\ 1 \\ 1 \\ 0 \\ 0 \\ 0 \end{Bmatrix} \sigma_w \tag{1.2.2}$$

where,

$\boldsymbol{\sigma}'$: Effective stress

σ_w : Pore water pressure

$\mathbf{m} = \{1,1,1,0,0,0\}^T$

The effective stress, $\boldsymbol{\sigma}'$ above can be expressed as,

$$\boldsymbol{\sigma}' = \mathbf{D}\boldsymbol{\varepsilon} = \mathbf{DBd} \tag{1.2.3}$$

where,

$\mathbf{D}$: Stiffness matrix of material

$\boldsymbol{\varepsilon}$: Elastic strain

$\mathbf{B}$: Strain-displacement relationship matrix

$\mathbf{d}$: Displacement

Also, the pore water pressure at any point inside an element, σ_w can be expressed as,

$$\sigma_w = \mathbf{N}_w \mathbf{p} \tag{1.2.4}$$

where,

$\mathbf{N}_w$: Element shape function for pore water pressure

$\mathbf{p}$: Nodal pore water pressure

Thus, Eq. (1.2.2) is rewritten as,

$$\boldsymbol{\sigma} = \mathbf{DBd} + \mathbf{mN}_w \mathbf{p} \tag{1.2.5}$$

By substituting Eq. (1.2.5) into Eq. (1.2.1) and using $\delta\boldsymbol{\varepsilon}^T\boldsymbol{\sigma} = \delta\mathbf{d}^T\mathbf{B}^T\boldsymbol{\sigma}$, the virtual work equation is expressed in terms of the virtual displacement, ($\delta\mathbf{d}^T$) as Eq. (1.2.6).

$$\begin{aligned} W_{\text{int}} &= \delta\mathbf{d}^T\left[\int_V \left(\mathbf{B}^T\mathbf{DBd} + \mathbf{BmN}_w\mathbf{p}\right)dV\right] \\ &= \delta\mathbf{d}^T\left[\mathbf{Kd} + \mathbf{Cp}\right] \end{aligned} \tag{1.2.6}$$

where, $\mathbf{K} = \int_V \mathbf{B}^T\mathbf{DB}dV$ and $\mathbf{C} = \int_V \mathbf{B}^T\mathbf{mN}_w dV$.

The external virtual work done by surface force and body force is as follows:

$$W_{ext} = \delta\mathbf{d}^T\mathbf{f}_{body} + \delta\mathbf{d}^T\mathbf{f}_{surface} = \delta\mathbf{d}^T\mathbf{F} \tag{1.2.7}$$

Eq. (1.2.6) and Eq. (1.2.7) must be in equilibrium. Under such condition, the following equilibrium equation from the physical point of view is obtained by applying the principle of virtual work:

$$\mathbf{Kd} + \mathbf{Cp} = \mathbf{F} \tag{1.2.8}$$

As mentioned above, in order to perform the analysis of fully coupled physical and flow problems, the flow equilibrium equation is additionally required in addition to the physical equilibrium equation.

In Figure 1.2.1, Q_{int} is the inflow flux into the specimen volume per unit time, and v_x, v_y and v_z represent the flow velocities in individual directions. The inflow flux is expressed as,

$$Q_{\text{int}} = v_x dydz + v_y dxdz + v_z dxdy + q_{\text{ext}} = V\left(\frac{v_x}{dx} + \frac{v_y}{dy} + \frac{v_z}{dz}\right) + q_{\text{ext}} \tag{1.2.9}$$

Also the outflow flux is as follows:

$$\begin{aligned} Q_{\text{out}} &= \left(v_x + \frac{dv_x}{dx}dx\right)dydz + \left(v_y + \frac{dv_y}{dy}dy\right)dxdz + \left(v_z + \frac{dv_z}{dz}dz\right)dxdy \\ &= V\left(\frac{v_x}{dx} + \frac{v_y}{dy} + \frac{v_z}{dz}\right) + V\left(\frac{dv_x}{dx} + \frac{dv_y}{dy} + \frac{dv_z}{dz}\right) \end{aligned} \tag{1.2.10}$$

Based on the assumption that water is incompressible and the soil is fully saturated, the difference between the inflow flux and outflow flux can be viewed to have been caused from the change in the volume of the specimen with time. Such relationship can be formulated as follows:

$$V\left(\frac{dv_x}{dx} + \frac{dv_y}{dy} + \frac{dv_z}{dz}\right) - q_{\text{ext}} = -\frac{d\Delta V}{dt} \tag{1.2.11}$$

Dividing the left and right sides of the above equation by the total volume, V, it can be transformed to express the flux per unit volume.

$$\frac{dv_x}{dx} + \frac{dv_y}{dy} + \frac{dv_z}{dz} - \frac{d\varepsilon_v}{dt} = \frac{q_{\text{ext}}}{V} \tag{1.2.12}$$

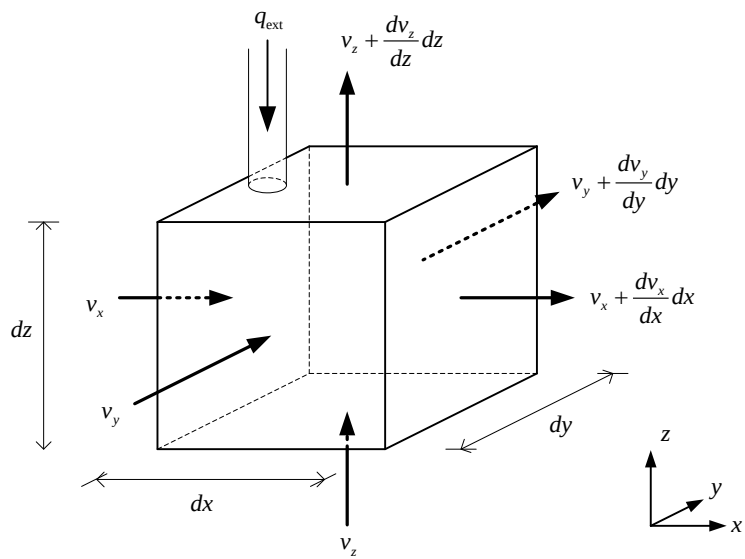

Figure 1.2.1 Inflow and outflow fluxes in the volume of specimen

The principle of virtual work is used to integrate the internal virtual work per unit volume, $\delta\mathbf{p}^T\mathbf{q}_{\text{int}}$ with respect to the total volume of the specimen.

$$W_{\text{int}} = \int_V \delta\nabla(p)^T v + \delta p^T \frac{d\varepsilon_v}{dt} dV \tag{1.2.13}$$

Substituting $\delta\nabla(p)^T = \delta\mathbf{p}^T\mathbf{B}_w^T$, $\delta p^T = \delta\mathbf{p}^T\mathbf{N}_w^T$ and $\varepsilon_v = \mathbf{m}^T\mathbf{B}\mathbf{d}$ into Eq. (1.2.13) gives,

$$\begin{aligned} W_{\text{int}} &= \delta\mathbf{p}^T \int_V \frac{1}{\gamma_w}\mathbf{B}_w^T\boldsymbol{\alpha}\mathbf{B}_w\mathbf{p} + \frac{1}{dt}\mathbf{N}_w^T\mathbf{m}^T\mathbf{B}\mathbf{d}\,dV \\ &= \delta\mathbf{p}^T\left(\frac{1}{dt}\mathbf{C}^T\mathbf{d} + \mathbf{S}\mathbf{p}\right) \end{aligned} \tag{1.2.14}$$

where, $\mathbf{C}^T = \int_V \mathbf{N}_w^T\mathbf{m}^T\mathbf{B}dV$ and $\mathbf{S} = \frac{1}{\gamma_w}\int_V \mathbf{B}_w^T\boldsymbol{\alpha}\mathbf{B}_w\,dV$

The external virtual work is as follows:

$$W_{\text{ext}} = \delta \mathbf{p}^T \mathbf{Q} \tag{1.2.15}$$

Eq. (1.2.6) and Eq. (1.2.7) must be in equilibrium. Under such condition, the following equilibrium equation from the physical point of view is obtained by applying the principle of virtual work:

$$\frac{1}{dt}\mathbf{C}^T \mathbf{d} + \mathbf{S}\mathbf{p} = \mathbf{Q} \tag{1.2.16}$$

Eq. (1.2.8) and Eq. (1.2.16) can be expressed in difference equations with respect to time for the increment from time t to $t \to t + \Delta t$.

$$\mathbf{K}\Delta\mathbf{d} + \mathbf{C}\left(\theta\Delta\mathbf{p} + \mathbf{p}_0\right) = \Delta\mathbf{F}$$

$$\mathbf{C}^T\Delta\mathbf{d} + \Delta t\mathbf{S}\left(\theta\Delta\mathbf{p} + \mathbf{p}_0\right) = \Delta t\mathbf{Q}$$

The above equations can be rewritten in a matrix form.

$$\begin{bmatrix} \mathbf{K} & \mathbf{C} \\ \mathbf{C}^T & \theta\Delta t\mathbf{S} \end{bmatrix} \begin{Bmatrix} \Delta\mathbf{d} \\ \Delta\mathbf{p} \end{Bmatrix} = \begin{Bmatrix} \Delta\mathbf{F} - \mathbf{C}\mathbf{p}_0 \\ \Delta t\left(\mathbf{Q} - \mathbf{S}\mathbf{p}_0\right) \end{Bmatrix}$$

SoilWorks internally uses $\theta = 1$ applying the backward difference equation.

1.3 Properties of Consolidation Elements

The important variables commonly sought in the finite element solution of consolidation analysis are the displacement and pore water pressure. Like incremental displacements are related to nodal displacements through an interpolation function, incremental pore water pressures are also related to nodal pore water pressures through an interpolation function in a similar way.

$$\Delta p = \mathbf{N}_w \Delta \mathbf{p}^{\text{nodal}} \tag{1.3.1}$$

From the above relationship equation, the left side represents the incremental pore water pressure, and the right side represents the interpolation function of each pore water pressure and the nodal incremental pore water pressure. SoilWorks assumes that the interpolation function of pore water pressure is identical to that of displacement.

In consolidation analysis, elements retain the nodal displacement degrees of freedom together with the additional degree of freedom for pore water pressure. Consolidation analysis in SoilWorks assumes that all elements retain the degree of freedom for pore water pressure unless two boundary conditions (non-consolidation condition and draining condition) are defined. As such, if elements are not expected to become subjected to consolidation, for instance, embankment materials, then a non-consolidation condition needs to be defined as shown in the Figure 1.3.1 so that they act as general structural elements. Also if a draining condition exists in the consolidation elements, the drainage boundary condition must be defined. Once consolidation analysis is carried out with proper boundary conditions, the excess pore water pressures must become “0” in the regions where non-consolidation and draining conditions are assigned.

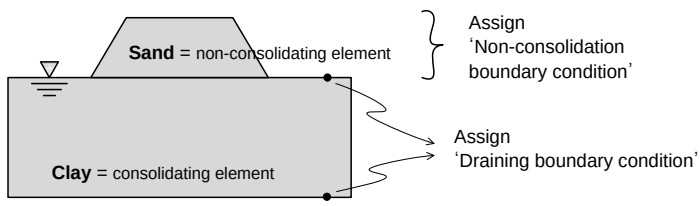

Figure 1.3.1 Boundary condition for consolidation elements

Elements that can be presently used as consolidation elements are plane strain elements (3-node, 6-node, 4-node and 8-node). Detail descriptions for the degrees of freedom for displacements and pore water pressures for each element and the integration method are outlined below.

1.3.1 Degrees of Freedom for Plane Strain Elements

In case of higher order elements, excess pore water pressure between nodes is linearly interpolated to generate stress analysis results. These dummy nodes, which are intended for extracting excess pore water pressures, do not exist in analysis (see Figure 1.3.2). All the nodes producing excess pore water pressures in consolidation analysis are located at corners, and a linear function is used to interpolate the pressures in the elements. This is known to be appropriate in reflection of the characteristic of water pressure distribution.

Triangular elements

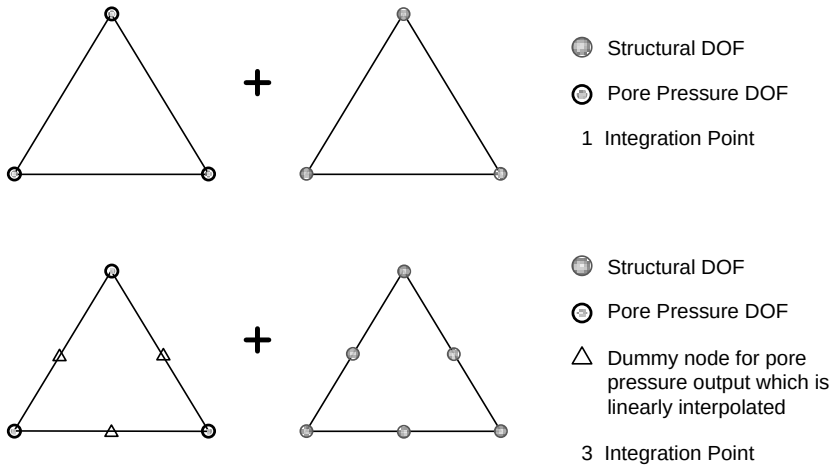

Figure 1.3.2 DOF for lower order 3-node and higher order 6-node triangular elements

Quadrilateral elements

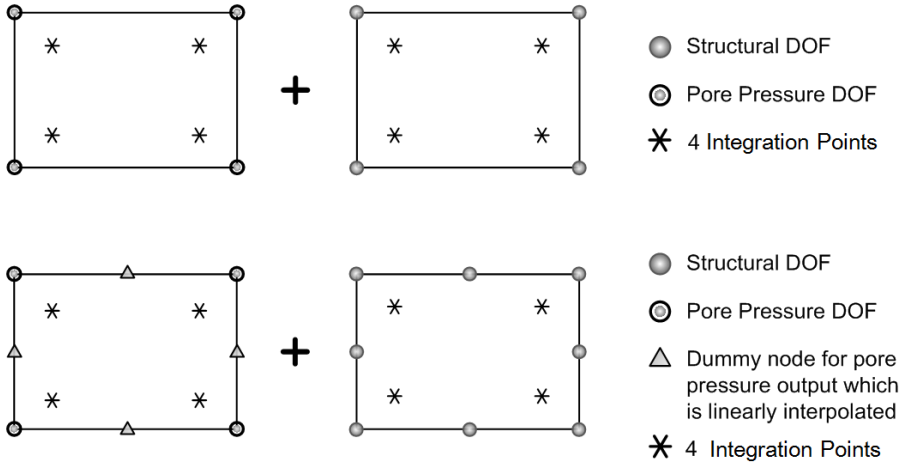

Figure 1.3.3 DOF for lower order 4-node and higher order 8-node quadrilateral elements

1.4 Cautionary Points for Consolidation Analysis

1.4.1 Time and Loading Input

In consolidation analysis, appropriate times for loading additional loads and loading distribution are carried out by entering the following times and load factors:

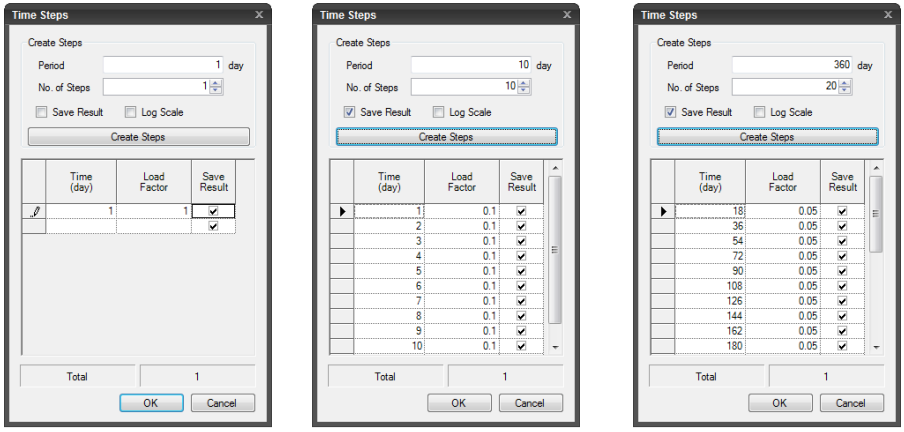

(a) Initial load (b) Additional load (c) Long-term load placement

Figure 1.4.1 input dialog for times and load factors

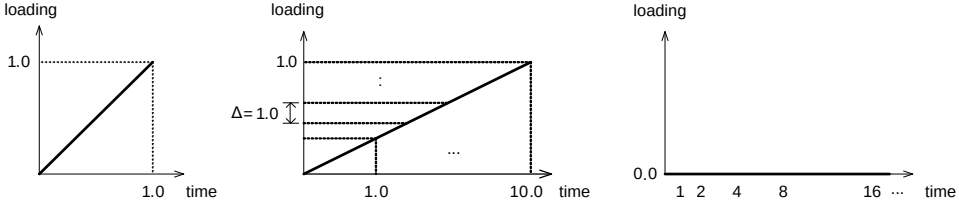

(a) Initial load (b) Additional load (c) Long-term load placement

Figure 1.4.2 Time and load graphs

In case the Modified Cam-Clay material model is used in consolidation analysis, an initial analysis must be performed for initial loads such as self weight. Because the analysis is intended to define the initial stress within the general range of linearity, the load is immediately applied in one time step as shown in the Figure 1.4.2 (a) Initial Load.

When additional loads are loaded for consolidation in construction stages, the total additional load is loaded at appropriate intervals over the total time as shown in the above Figure 1.4.2 (b) Additional loads. Figure 1.4.2 (b) shows an example in which additional loads are loaded at 10 equal intervals over a total of 10 days. The sum of the total load factors must be equal to 1.0. If an additional load suddenly becomes large or the analysis time is inappropriate, convergence in consolidation analysis may not be attainable. In such cases, the time step needs to be reasonably reduced and the load factor needs to be set smaller in order to improve the convergence. Of course the total load factor still must be 1.0 unless especially intended for other purposes.

Once the embankment has been completed, analysis for a long-term load placement is carried out during which only time elapses. Figure 1.4.2 (c) shows that only time is specified without adding external loads in construction stages. Due to the characteristics of consolidation analysis, stress variations in the initial stages are rather drastic. Figure 1.4.2 (c) shows that the initial time steps start with small intervals and gradually increase to larger intervals to achieve a better convergence and faster analysis speed simultaneously.

Chapter 2

1-Dimensional Theoretical Analysis

2.1 Introduction

This chapter describes the theoretical background to the analysis of soft ground. The following functions are available in the analysis of soft ground for calculating 1-dimensional consolidation settlement:

- ✓ Calculation of consolidation settlement for soft cohesive soil (Cc method, Mv method & Δe method)
- ✓ Calculation of settlement and degree of consolidation reflecting loading stages
- ✓ Calculation of strength increase by loading stages
- ✓ Calculation of stress increase by Boussinesq's equation
- ✓ Calculation of immediate settlement for sandy soil (De Beer method & B.K. Hough method)
- ✓ Calculation of secondary consolidation settlement
- ✓ Application of external loads (point load, line load, strip load & rectangular load)
- ✓ Calculation of soil coefficients by ground layers using e-logP, logMv-logP and logCv-logP curves
- ✓ Overconsolidation and normal consolidation analyses
- ✓ Settlement reduction reflecting SCP or GCP
- ✓ Smear effect and well resistance considered

2.2 Settlement Calculation Methods

2.2.1 Consolidation Settlement of Cohesive Soil

1) C_c method

$$S = \frac{\Delta e}{1+e_0} H \tag{2.2.1}$$

where,

S	: Consolidation settlement
H	: Thickness of consolidation layer
e_0	: Initial void ratio and
Δe	: Change in void ratio

For normal consolidation clay ($P_0 \geq P_c$)

$$\Delta e = C_c \cdot \log\left(\frac{P_0 + \Delta P}{P}\right) \tag{2.2.2}$$

$$S = \frac{C_c \cdot H}{1+e_0} \cdot \log\left(\frac{P_0 + \Delta P}{P}\right) \tag{2.2.3}$$

For overconsolidation clay ($P_0 < P_c$)

For $P_0 < P_0 + \Delta P < P_c$

$$\Delta e = C_s \cdot \log\left(\frac{P_0 + \Delta P}{P_0}\right) \tag{2.2.4}$$

$$S = \frac{C_s \cdot H}{1+e_0} \cdot \log\left(\frac{P_0 + \Delta P}{P_0}\right) \tag{2.2.5}$$

For $P_0 < P_c < P_0 + \Delta P$

$$\Delta e = \Delta e_1 + \Delta e_2 = C_s \cdot \log \frac{P_c}{P_0} + C_c \cdot \log\left(\frac{P_0 + \Delta P}{P_c}\right) \tag{2.2.6}$$

$$S = \frac{C_s \cdot H}{1+e_0} \cdot \log \frac{P_c}{P_0} + \frac{C_c \cdot H}{1+e_0} \cdot \log\left(\frac{P_0 + \Delta P}{P_c}\right) \tag{2.2.7}$$

where,

S	: Consolidation settlement
H	: Thickness of consolidation layer
C_s	: Swelling index
P_0	: Effective overburden pressure
P_c	: Preconsolidation load
e_0	: Initial void ratio
C_c	: Compression index
ΔP	: Vertical stress increment due to embankment or external loads

2) Δe method

$$S = \frac{e_0 - e_1}{1+e_0} H \tag{2.2.8}$$

where,

S	: Consolidation settlement
H	: Thickness of consolidation layer
e_0	: Initial void ratio (void ratio for effective overburden pressure P_0)
e_1	: Void ratio after consolidation (void ratio for effective overburden pressure $P_0 + \Delta P$)
ΔP	: Vertical stress increment due to embankment or external loads

3) M_v method

$$S = M_v \cdot \Delta P \cdot H \tag{2.2.9}$$

where,

S : Consolidation settlement

H : Thickness of consolidation layer

M_v : Volume compressibility coefficient

(for $P_0 + \frac{\Delta P}{2}$ in $\log M_v - \log P$ curve)

ΔP : Vertical stress increment due to embankment or external loads

The characteristics and the range of applications of the above consolidation settlement formulas are listed in Table 2.2.1.

Table 2.2.1 Characteristics and range of applications of consolidation settlement formulas

Consolidation settlement calculation method	Characteristics	Range of applications
Δe method	The difference in gradient or void ratio is relatively small, but the error in absolute value of void ratio is rather large. When a number of consolidation test results are collected, $e - \log P$ curves become scattered lines, leading to difficulty in determining one planar curve.	Hardly used in actual design
M_v method	If the coefficient of volume compressibility is used, the gradient distribution is large in overconsolidated zones, but is small in normally consolidated zones; thereby resulting in one straight line with reasonable results overall.	Used for areas abundant in test results or wide areas
C_c method	The compressibility index is defined as the linear gradient of $e - \log P$ curve. However, using the average values may be difficult and overestimated because the gradient is not a straight line but a reversed S curve or the void ratio is inconsistent. Estimating C_c by depths is difficult.	Used when consolidation test cases are few or none and when an approximate settlement calculation using physical properties is performed.

2.2.2 Settlement of Sandy Soil

Settlements occurring in sandy soils are immediate settlements, which take place immediately upon loading. Various methods have been proposed for calculating immediate settlements, which include Schmertmann, Meyerhof, Peck, De Beer and Parry. Different methods will lead to different settlements.

Since it is difficult to sample and mold undisturbed sandy soil specimens, obtaining accurate mechanical properties is not so trivial. As such, the settlements of sandy soils will be calculated by the methods of De Beer and B.K.Hough chart, which use the standard penetration test values (N).

1) De Beer method

$$S_i = 0.4\frac{P_0}{N} \cdot H \cdot \log\left(\frac{P_0 + \Delta P}{P_c}\right) \tag{2.2.10}$$

where,

N	: Standard penetration test value
H	: Thickness of consolidation layer
P_0	: Effective overburden pressure
ΔP	: Vertical stress increment due to embankment or external loads

2) B.K.Hough chart method

The B.K.Hough chart method estimates void ratio using Figure 2.2.1 or Table 2.2.2.

Table 2.2.2 Void ratios according to consolidation pressures (B.K.Hough chart method)

Consolidation pressure (P)	Void ratio e				
	Very loose (N=0~4)	Loose (N=4~10)	Medium dense (N=10~30)	Dense (N=30~50)	Very dense (N=50~100)
0.2	0.967	0.780	0.586	0.490	0.395
0.3	0.947	0.760	0.578	0.484	0.392
0.5	0.922	0.742	0.567	0.477	0.388
1.0	0.889	0.714	0.554	0.467	0.383
2.0	0.855	0.688	0.540	0.457	0.378
3.0	0.836	0.678	0.532	0.451	0.375
5.0	0.811	0.662	0.521	0.443	0.372
10.0	0.778	0.640	0.507	0.433	0.367
20.0	0.744	0.621	0.493	0.423	0.362
30.0	0.725	0.611	0.485	0.417	0.359
50.0	0.700	0.600	0.475	0.410	0.355

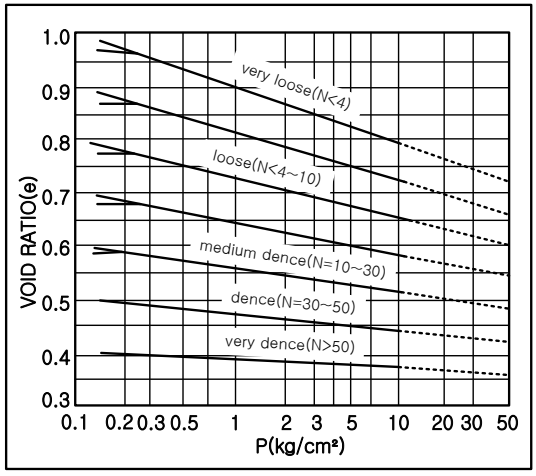

Figure 2.2.1 $e-\log P$ curve (B.K.Hough chart method)

2.2.3 Rebound of Cohesive Soil

When the embankment or external load is removed, cohesive soil will rebound, and the rebound calculations according to different settlement calculation methods are as follows:

1) C_c Method

In the C_c method, the rebound is calculated using the removed stress, ΔP and the slope, C_s of the $e - \log P$ curve after the removal (Figure 2.2.2).

$$S_h = \frac{C_s}{1+e_1} \cdot H_b \cdot \log_{10}\left(\frac{P_2 + \Delta P}{P_2}\right) \tag{2.2.11}$$

where,

C_s : Removal factor

e_1 : Void ratio immediately before removal

H_b : Layer thickness immediately before removal (initial layer thickness, H_0 subtracted by the settlement up to the stage immediately before removal)

P_2 : Stress after removal (= $P_1 - \Delta P$)

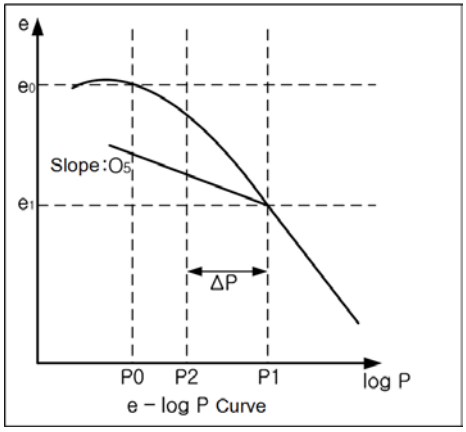

Figure 2.2.2 Definition of removal factor in the C_c method

2) Δe Method

In the Δe method, the rebound is calculated using the void ratios before and after removal of the load and the slope, R of the $e - \log P$ curve after the removal of the load (Figure 2.2.3).

$$S_h = \frac{e_2 - e_1}{1 + e_1} \cdot H_b \qquad (2.2.12)$$

where,

e_1 : Void ratio immediately before removal

e_2 : Void ratio after removal,

H_b : Layer thickness immediately before removal (initial layer thickness, H_0 subtracted by the settlement up to the stage immediately before removal)

P_2 : Stress after removal (= $P_1 - \Delta P$)

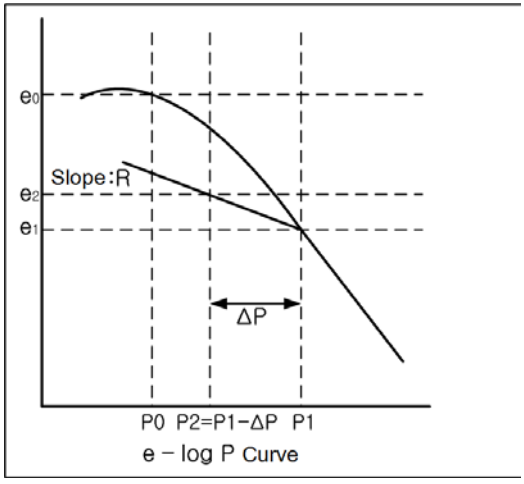

Figure 2.2.3 Definition of removal factor in the Δe method

3) M_v Method

In the M_v method, the rebound is calculated as follows:

$$S_h = M_{vr} \cdot \Delta P \cdot H_b \tag{2.2.13}$$

where,

M_{vr} : Removal factor

H_b : Layer thickness immediately before removal (initial layer thickness, H_0 subtracted by the settlement up to the stage immediately before removal)

The removal factor is always considered to retain the positive (+) sign. If the removal factor is zero, it is assumed that no rebound takes place upon unloading. In sandy soils, the rebound is not calculated.

2.2.4 Secondary Consolidation Settlement

Secondary consolidation is referred to as the phenomenon of compression, which continues after excess pore water pressure has completely dissipated. In Figure 2.2.4, the slope of the secondary consolidation is almost linear after the primary consolidation has completed. This slope can be used to obtain the coefficient of the secondary consolidation, C_a .

$$C_a = \frac{\Delta H / H_p}{\Delta \log_{10} t} \tag{2.2.14}$$

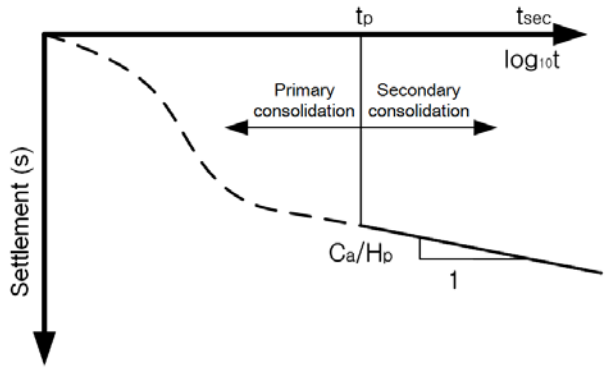

Figure 2.2.4 Coefficient of secondary consolidation

In general, the coefficient of secondary consolidation used corresponds to the natural water content from NAVFAC DM 7.2. The secondary consolidation settlement is calculated as follows:

$$S_2 = C_a \cdot H_p \cdot \log \frac{t_s}{t_p} \tag{2.2.15}$$

where,

S_2 : Secondary consolidation settlement

C_a : Coefficient of secondary consolidation

H_p : Thickness of consolidation layer excluding the primary consolidation settlement from the initial thickness

t_s : Assumed secondary consolidation

t_p : Time at which the primary consolidation ended

2.3 Calculation of the Effective Overburden Pressure and the Increase in Vertical Stress

2.3.1 Effective Overburden Pressure

For the ground strata above the groundwater level, the wet unit weight is used. For the ground strata below the groundwater level, the submerged unit weight is used because the effective stress is calculated. As shown in Figure 2.3.1, the effective overburden pressure (the pressure due to the initial ground weight prior to application of loading) at the center of soil layer i is calculated as follows:

$$P_{0,i} = \gamma_1 H_1 + ... + \gamma_{i-1} H_{i-1} + \frac{1}{2}\gamma_i H_i \qquad (2.3.1)$$

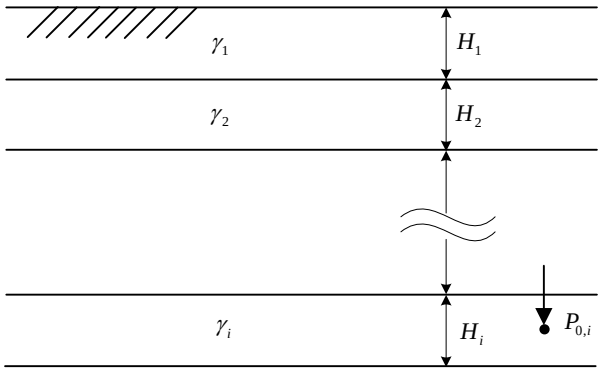

Figure 2.3.1 Effective overburden pressure

2.3.2 Embankment Load

The increase in the ground stress due to embankment loads is calculated by computing the incremental stress for an infinitesimal length between two adjacent points using the concept of strip load and summing the incremental stresses (Figure 2.3.2).

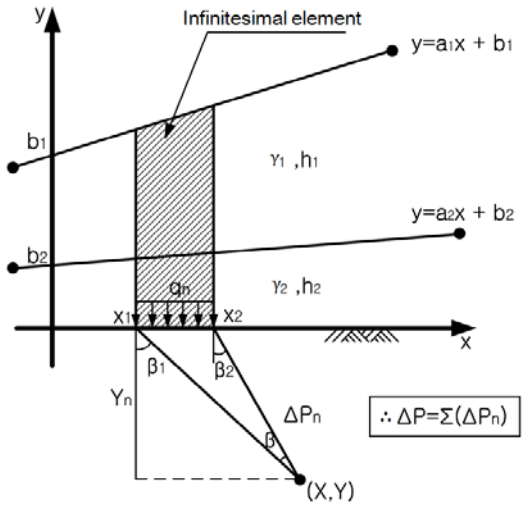

Figure 2.3.2 Ground stress due to embankment load

The load acting on the infinitesimal length, q_n becomes,

$$q_n = \gamma_1 h_1 + \gamma_2 h_2 + ... + \gamma_i h_i \tag{2.3.2}$$

The increase in the ground stress, ΔP_n at a specific point (x, y) due to the load q_n acting on an infinitesimal length is given by,

$$\Delta P_n = \frac{q_n}{\pi}\left[\sin\beta \cdot \cos\phi + \beta\right] \tag{2.3.3}$$

$$\Delta P = \Sigma\left[\Delta P_n\right] \tag{2.3.4}$$

where, $\beta = \beta_1 - \beta_2$, $\phi = \beta_1 + \beta_2$, $\beta_1 = \tan^{-1}\left(\frac{x - x_1}{Y_n}\right)$ and $\beta_2 = \tan^{-1}\left(\frac{x - x_2}{Y_n}\right)$

2.3.3 Point Load

As shown in Figure 2.3.3, Boussinesq proposed the following relationship of stress applied to a soil element in the ground when a point load, P is acting on the ground surface:

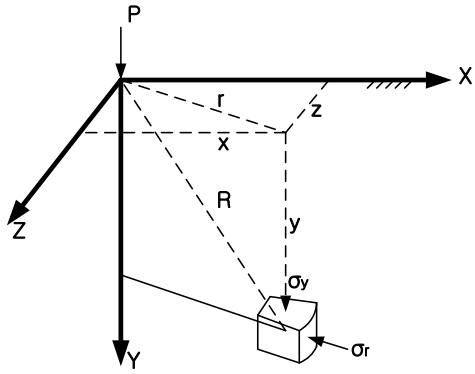

Figure 2.3.3 Stress in the ground due to a point load

$$\Delta P = \frac{3P}{2\pi}\frac{y^3}{R^5} = \frac{3P}{2\pi}\frac{y^3}{\left(r^2+y^2\right)^{5/2}} \tag{2.3.5}$$

where,

$$r = \sqrt{x^2+z^2} \quad \text{and} \quad R = \sqrt{x^2+y^2+z^2} = \sqrt{r^2+y^2} \tag{2.3.6}$$

2.3.4 Line Load

As shown in Figure 2.3.4, when a line load, q per unit length is applied to the ground surface, the incremental stress at a point in the ground is expressed as,

$$\Delta P = \frac{2qy^3}{\pi\left(x^2+y^2\right)^2} \tag{2.3.7}$$

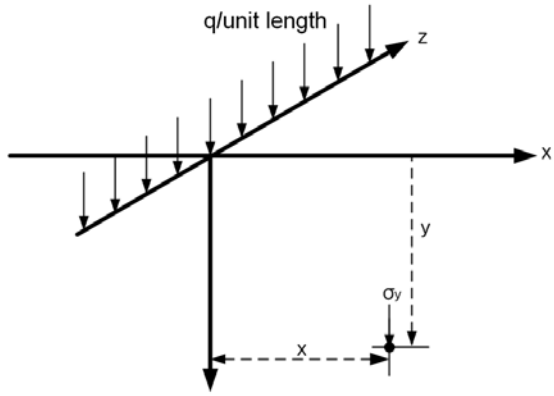

Figure 2.3.4 Stress in the ground due to a line load

2.3.5 Strip Load

Stress due to a strip load can be determined by integrating the stresses due to line loads over the strip width. The incremental stress due to a strip load is calculated as shown in Figure 2.3.5.

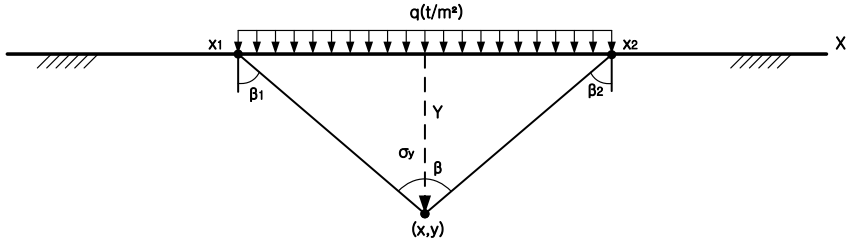

Figure 2.3.5 Stress in the ground due to a strip load

$$\begin{aligned}\Delta P &= \frac{2q}{\pi}\int_{x_1}^{x_2}\frac{y^3}{\left(x^2+y^2\right)^2}dx \\ &= \frac{2qy^3}{\pi}\left[\frac{1}{2y^2}\left(\frac{x}{x^2+y^2}+\frac{1}{y}\cdot\tan^{-1}\frac{x}{y}\right)\right]_{x_1}^{x_2} \\ &= \frac{q}{\pi}\left[\left(\frac{x_2 y}{x_2^2+y^2}+\tan^{-1}\frac{x_2}{y}\right)-\left(\frac{x_1 y}{x_1^2+y^2}+\tan^{-1}\frac{x_1}{y}\right)\right] \\ &= \frac{q}{\pi}\left(\frac{x_2 y}{R_2^2}-\frac{x_1 y}{R_1^2}+\beta_2-\beta_1\right)\end{aligned} \tag{2.3.8}$$

Rewriting the above equation using $R_1^2 = x_1^2 + y^2$ and $R_2^2 = x_2^2 + y^2$ gives,

$$\begin{aligned}\Delta P &= \frac{q}{\pi}\left(\sin\beta_2\cos\beta_2-\sin\beta_1\cos\beta_1+\beta_2-\beta_1\right) \\ &= \frac{q}{\pi}\left[\sin\left(\beta_2-\beta_1\right)\cdot\cos\left(\beta_2+\beta_1\right)+\beta_2-\beta_1\right]\end{aligned} \tag{2.3.9}$$

Using $\beta = \beta_1 - \beta_2$, $\phi = \beta_1 + \beta_2$, $\beta_1 = \tan^{-1}\left(\frac{x-x_1}{Y}\right)$ and $\beta_2 = \tan^{-1}\left(\frac{x-x_2}{Y}\right)$, the equation becomes,

$$\Delta P = \frac{q}{\pi}\left[\sin\beta\cdot\cos\phi+\beta\right] \tag{2.3.10}$$

2.3.6 Rectangular Load

The increase in the soil stress in the ground when a rectangular load is acting on the ground surface as shown in Figure 2.3.6 is given by,

$$\Delta P = \frac{2q}{\pi}\left[\tan^{-1}\frac{ab}{yR_3}+\frac{aby}{R_3}\left(\frac{1}{R_1^2}+\frac{1}{R_2^2}\right)\right] \tag{2.3.11}$$

where, $R_1 = \sqrt{a^2+y^2}$, $R_2 = \sqrt{b^2+y^2}$ and $R_3 = \sqrt{a^2+b^2+y^2}$ (2.3.12)

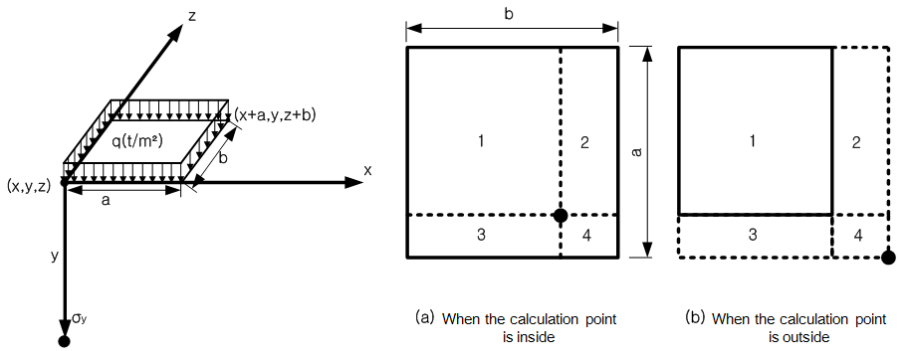

Figure 2.3.6 Stress in the ground due to a rectangular load

When the calculation point is inside the rectangle, the rectangle is divided into four rectangles relative to the calculation point, and the incremental stress is calculated by summing up the stress of each division.

$$\Delta P \text{ (Inside)} = \Delta P_1 + \Delta P_2 + \Delta P_3 + \Delta P_4 \tag{2.3.13}$$

When the calculation point is outside the loaded rectangle denoted as the area 1 in Figure 2.3.6 (b), four imaginary rectangles beyond the loaded area are constructed to extend to the calculation point, and the incremental stress is calculated for the original rectangle.

$$\Delta P \text{ (Outside)} = \Delta P_{1+2+3+4} - \Delta P_{2+4} - \Delta P_{3+4} + \Delta P_4 \tag{2.3.14}$$

2.3.7 Calculation of Increase in Ground Stress

The increase in the effective vertical stress due to a load acting on the ground surface can be calculated by the following two methods:

Calculation at the center of a layer

This method uses the incremental stress at the center of each settlement layer.

Calculation by the Simpson method

The vertical stresses at the top, middle and bottom surfaces of a layer are individually calculated, and the incremental stress at the center of each layer is calculated by the Simpson method.

$$\Delta P = \frac{1}{6}\left(\Delta P_t + 4 \cdot \Delta P_m + \Delta P_b\right) \qquad (2.3.15)$$

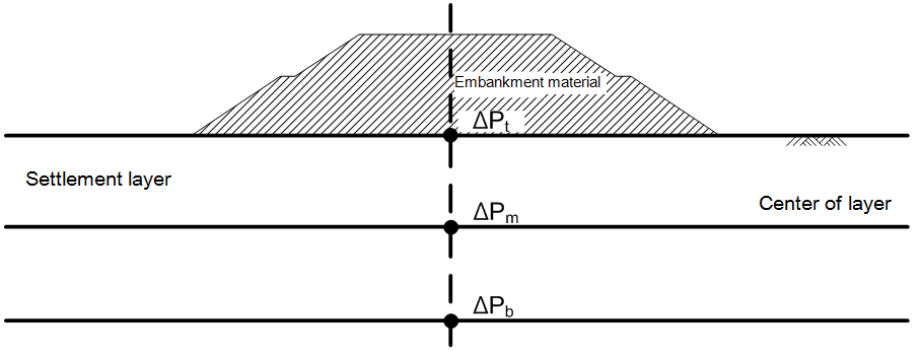

Figure 2.3.7 Calculation of incremental stress using the Simpson method

2.3.8 Loading Distance of Embankment Load

The loading distance (z) for calculating the increase in the ground stress due to an embankment load can be defined by the distance from the bottom of the embankment or from the initial ground surface. In case of a number of staged embankment loads, the loading distances can be defined as follows:

1) Loading Distance from the Bottom of Embankment

The loading distance is taken as the distance from the bottom of embankment at each stage to the point of calculating the increase in the ground stress.

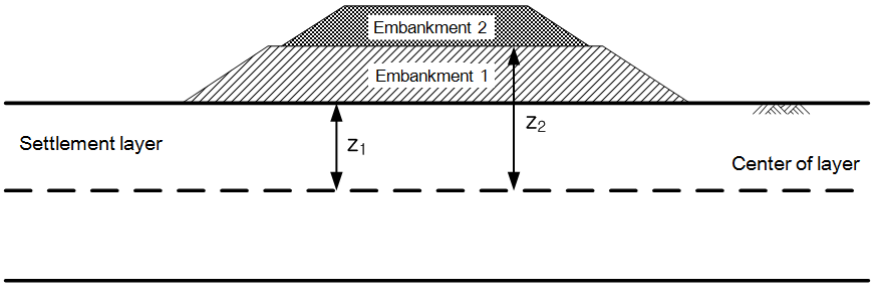

Figure 2.3.8 Calculation of loading distance from the bottom of embankment

2) Loading Distance from the Initial Ground Surface

The loading distance is taken as the distance from the initial ground surface to the calculation point $(z_1 = z_2)$ of the increase in the ground stress irrespective of the embankment stages.

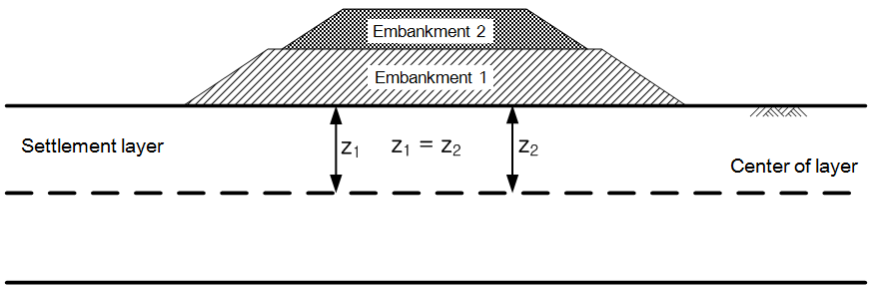

Figure 2.3.9 Calculation of loading distance from the initial ground surface

2.4 Calculation of the Degree of Consolidation Relative to Settlement Time

2.4.1 Consolidation Time for Unimproved Soil

Embankment on roadways actually results in two-dimensional or three-dimensional consolidation. However, the calculation of the consolidation time, which depends on the degree of consolidation, is based on the Terzaghi's one-dimensional consolidation theory. The consolidation time is calculated considering the degree of consolidation and the time factor for instantaneous loading.

$$t = \frac{T_v \cdot D_d^2}{C_v} \qquad (2.4.1)$$

where,

t	: Consolidation time
D_d	: Drainage distance of pore water
T_v	: Time factor
C_v	: Coefficient of consolidation.

The time factor, T_v is defined by the Terzaghi's simple equations.

$$T_v = \frac{\pi}{4}\left(\frac{U}{100}\right)^2 \qquad \text{: for 0\% < U < 53\%} \qquad (2.4.2)$$

$$T_v = 1.781 - 0.933 \cdot \log(100 - U) \qquad \text{: for 53\% < U < 100\%} \qquad (2.4.3)$$

2.4.2 Conversion of the Thickness of Consolidation Layer

If the coefficient of consolidation, C_v is different for each layer, the average degree of consolidation of all the layers is calculated using the converted thickness, H' and the converted consolidation coefficient, C_v' obtained by the method of thickness conversion as follows:

$$H' = H_1\sqrt{\frac{C_v'}{C_{v1}}} + H_2\sqrt{\frac{C_v'}{C_{v2}}} + ... + H_n\sqrt{\frac{C_v'}{C_{vn}}} \qquad (2.4.4)$$

where,

H' : Converted thickness of consolidation layer

H_n : Thickness of the layer n before conversion

C_v' : Converted consolidation coefficient

C_{vn} : Coefficient of consolidation of the layer n before conversion

The converted consolidation coefficient, C_v', which becomes the reference, can be evaluated from one of the following three methods:

C_v' is taken as the average of all the layers' coefficients.

C_v' is taken as the C_v of the top layer.

C_v' is taken as the C_v of the bottom layer.

Different drainage boundaries can be specified for different layers, but all the layers constituting a converted layer must have an identical drainage boundary condition (single face or both faces). The drainage condition and the composition of converted layer of each layer in multilayered ground are illustrated in Figure 2.4.1.

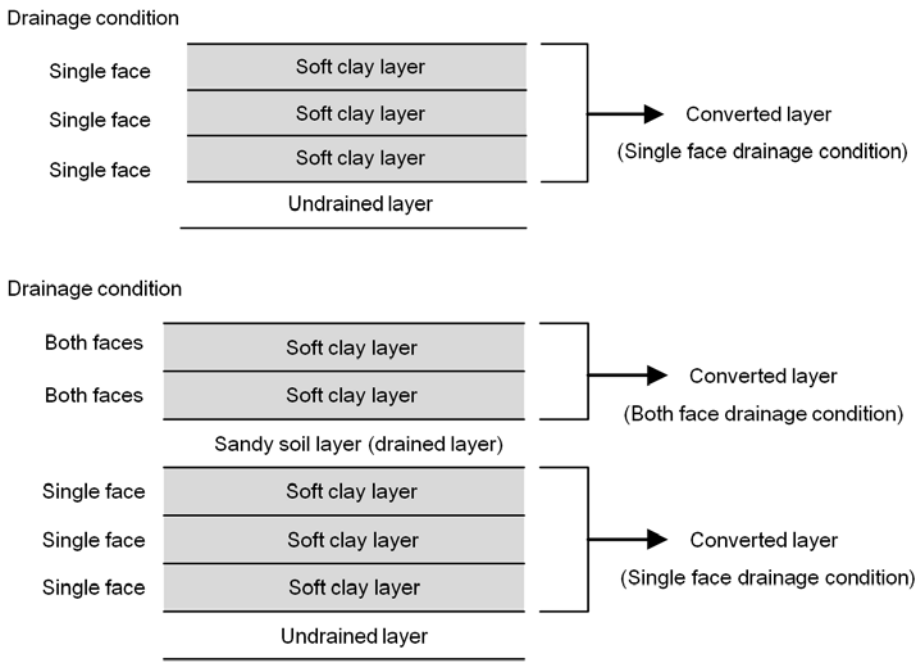

Figure 2.4.1 Drainage conditions and composition of converted layers in multilayered ground

When an unconsolidated clay layer exists within a number of consecutive soft clay layers, the unconsolidated layer may or may not be considered in the calculation of the converted thickness.

As shown in Figure 2.4.2, when a drainage layer exists at the bottom and a thin unconsolidated layer exists at the top, it is not recommended to consider single face drainage for the middle consolidated layers for the calculation of the converted thickness because of the existence of the top unconsolidated layer. In such a case, the settlement of the thin unconsolidated layer is not calculated, but the unconsolidated layer thickness should be included in the calculation of the converted layer thickness when calculating the converted drainage distance for the calculation of settlement time. Even when thin unconsolidated layers exist within the multiple layers of soft clay, it is desirable to reflect the thicknesses of the unconsolidated layers in the calculation of the converted layer thickness.

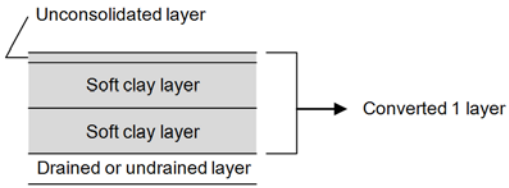

Figure 2.4.2 Thickness of unconsolidated layer reflected in the calculation of converted layer thickness

As shown in Figure 2.4.3, if the unconsolidated layer is relatively thicker than the consolidated layers, it is not desirable to reflect the thickness of the unconsolidated layer thickness in the calculation of the converted layer thickness.

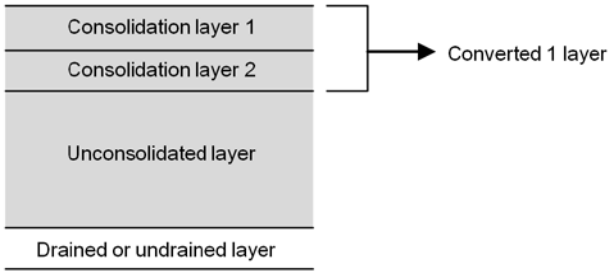

Figure 2.4.3 Thickness of unconsolidated layer not reflected in the calculation of converted layer thickness

2.4.3 Calculation of the Degree of Consolidation by Different Drainage Methods

2.4.3.1 Methods of Calculating the Degree of Consolidation

The theoretical equations for consolidation drainage commonly consider the effect of the drainage distance. Depending on the consideration of the smear effect that can occur during the construction of vertical drains and the well resistance that can occur during the drainage of consolidated water inside the vertical drains, the proposed equations differ by Barron (1948), Hansbo (1981), Yoshikuni (1979), Onoue (1988), etc.

The Hansbo's equation, which can consider both the smear effect and well resistance, is most widely used. SoilWorks supports the equations proposed by Barron, Hansbo and Yoshikuni.

1) Hansbo's Equation (1981)

Hansbo proposed the average degree of consolidation at a specific depth in order to consider the smear effect of ground disturbance during the construction of vertical drains and the well resistance of the drainage in the following equation:

$$U_h = 1 - \exp\left(\frac{-8T_h}{F}\right) \tag{2.4.5}$$

$$F = F(n) + F_s + F_r \tag{2.4.6}$$

$$T_h = \frac{C_h \cdot t}{d_e^2} \tag{2.4.7}$$

where,

U_h	: Average degree of consolidation in the horizontal direction
T_h	: Time factor in the horizontal direction
$F(n)$	: Effect of drainage spacing
F_s	: Smear effect
F_r	: Effect of well resistance
C_h	: Coefficient of consolidation in the horizontal direction
d_e	: Diameter of influence circle

Effect of drainage spacing, $F(n)$

$$F(n) = \ln(n) - \frac{3}{4} \quad \text{for} \quad n \geq 20 \tag{2.4.8}$$

$$F(n) = \frac{n^2}{n^2 - 1} \cdot \ln(n) - \frac{3n^2 - 1}{4n^2} \quad \text{for} \quad n < 20 \tag{2.4.9}$$

Smear effect, F_s

$$F_s = \left(\frac{k_h}{k_s} - 1\right) \cdot \ln\left(\frac{d_s}{d_w}\right) \tag{2.4.10}$$

Effect of well resistance, F_r

$$F_r = \pi z(2L - z)\frac{k_h}{q_w} \tag{2.4.11}$$

where,

$n = \dfrac{d_e}{d_w}$

d_e : Diameter of influence circle

d_w : Diameter of a vertical drain

k_h : Coefficient of permeability in the horizontal direction in undisturbed cohesive soil

k_s : Coefficient of permeability in the horizontal direction in the smear zone

d_s : Diameter of the smear zone around the drain ($d_s = 2d_m$)

d_m : Diameter of cone casing, q_w : Discharge capacity of drainage $\left(q_w = \dfrac{k_w \cdot \pi \cdot d_w^2}{4}\right)$

k_w : Coefficient of permeability of the vertical drain material

L : Length of drainage

($L = H$ for single face drainage, $L = H/2$ for double face drainage)

The average degree of consolidation for the entire layers simultaneously considering the degrees of consolidation in both vertical and horizontal directions is calculated as follows:

$$U_{vh} = 1 - (1 - U_h)(1 - U_v) \tag{2.4.12}$$

The equivalent coefficient of permeability can be applied to multilayered ground in the calculation of the degree of consolidation for horizontal drainage. If the thickness of each layer is denoted by $h_1, h_2, \ldots, h_n$, and the coefficient of permeability corresponding to each layer is denoted by $k_1, k_2, \ldots, k_n$, the equivalent coefficient of permeability in the horizontal direction is defined as,

$$k_h = \frac{1}{h}(k_1 h_1 + k_1 h_1 + \ldots + k_n h_n) = \frac{1}{h}\sum_{j=1}^{n}(k_j h_j) \tag{2.4.13}$$

2) Barron's Equation (1984)

Based on the Terzaghi's theory, Barron proposed that the average degree of consolidation for the entire layers would be calculated as follows under the equal strain consolidation condition:

$$U_h = 1 - \exp\left(\frac{-8T_h}{F(n)}\right) \tag{2.4.14}$$

$$F(n) = \frac{n^2}{n^2 - 1} \cdot \ln(n) - \frac{3n^2 - 1}{4n^2} \tag{2.4.15}$$

where,

$n = \dfrac{d_e}{d_w}$

$F(n)$: Effect of drainage spacing

d_e : Diameter of influence circle

d_w : Diameter of a vertical drain

3) Yoshikuni's Equation (1979)

Yoshikuni proposed the average degree of consolidation in the following equation, which considers only the well resistance:

$$U_h = 1 - \exp\left(\frac{-8T_h}{m}\right) \tag{2.4.16}$$

$$m = F(n) + 0.8L \tag{2.4.17}$$

$$F(n) = \frac{n^2}{n^2 - 1} \cdot \ln(n) - \frac{3n^2 - 1}{4n^2} \tag{2.4.18}$$

$$L = \frac{32}{\pi^2} \cdot \frac{k_h}{k_w} \cdot \left(\frac{H}{d_w}\right)^2 \tag{2.4.19}$$

where,

L : Well resistance factor

H : Length of drainage ($H/2$ for double face drainage)

4) Onoue's Equation (1988)

Onoue proposed the equations below, which would reflect the effects of smear zone and well resistance irrespective of permeability, using the drain resistance factor, L, which was proposed by Yoshikuni and Nakmodo (1974):

$$U_h = 1 - \exp\left(\frac{-8T_h}{F(n') + 0.8L}\right) \tag{2.4.20}$$

$$F(n') = \frac{(n')^2}{(n')^2 - 1} \cdot \ln(n') - \frac{3(n')^2 - 1}{4(n')^2} \tag{2.4.21}$$

$$L = \frac{32}{\pi^2} \cdot \frac{k_h}{k_w} \cdot \left(\frac{H}{d_w}\right)^2 \tag{2.4.22}$$

where,

$n' = nS^{\eta-1}$

$\eta = \frac{k_h}{k_s}$

$S = \frac{d_s}{d_w}$

H : Length of drainage ($H/2$ for double face drainage)

2.4.3.2 Effect of Vertical Drain Holes

1) Smear Zone

When a mandrel penetrates into the ground, the soil is disturbed and hence the coefficient of consolidation is reduced resulting in the delay of consolidation. The zone in which the soil becomes disturbed is called a smear zone, which depends on the size and shape of casing, the structure and type of soil and the type of drainage. By introducing certain design parameters into the theoretical equations, the level of delay in consolidation due to the smear effect can be reflected in the design.

The range of the smear zone (d_s) and the reduction ratio of permeability coefficient (k_s/k_h) vary with different proposers.

Table 2.4.1 Range of a smear zone (d_s)

Proposer	Range of smear zone
Jamiolkowski (1985)	$(2.5 \sim 3.0)d$
Hunt (1986)	$(1.3 \sim 1.5)d$
Hansbo (1987)	$2.0d$
Bergado (1991)	$2.0d$

d : Diameter of drainage material or casing

Table 2.4.2 Reduction ratio of permeability coefficient (k_s/k_h)

Proposer	Reduction ratio of permeability coefficient
Jamiolkowski (1985)	0.50~0.67
Onoue (1991)	0.20~0.67
Bergado (1991)	0.57

2) Well Resistance

As the consolidation progresses, the discharge capacity of the vertical drainage is reduced, which in turn delays the consolidation. Hansbo realized that no drainage would have an infinite coefficient of permeability in the length direction, and ignoring the well resistance would result in an under-design. It is necessary to minimize the well resistance in the long run by identifying the influential factors.

Factors influencing well resistance

- ✓ Bending and folding of PBD (Plastic Board Drain)
- ✓ Creep deformation of PBD filter due to soil pressure
- ✓ Change in hydraulic gradient

Cases of significant well resistance

- ✓ When the abundance of dissolved air is present in pore water
- ✓ When the coefficient of permeability of the soil is significant
- ✓ When the PBD is long
- ✓ When the use of PBD has been long

2.4.3.3 Types of Vertical Drainage Methods

Since Porter introduced the sand drain method in the 1930's, rapid progress has been made in introducing new theories and construction techniques of vertical drain methods from the late 1940's. In 1936, Kjellman et al. introduced a paper drain made out of cardboard and in 1978 the pack drain method was developed in Japan, which improved the ground by using the sand drainage together with net.

Vertical drains are inserted at close spacing into the cohesive soil layers and hence the pore water can flow into the permeable layers. The installation of vertical drains reduces the drainage length and consequently accelerates the consolidation settlement and shortens the time for ground stabilization. Different types of vertical drains include Sand Drain, Pack Drain, Paper Drain, Sand Compaction Pile, Gravel Compaction Pile, Cylindrical Drain, etc., and their basic principles are identical.

1) Sand Drain Method

In the sand drain method, sand columns are vertically driven into the ground to let the pore water out and thus shorten the drain length, thereby accelerating the consolidation. When the soft ground is loaded by an embankment, the loading induces excess pore water pressure. The pore water then discharges due to the hydraulic gradient, which results in consolidation. When a soft ground layer is thick and no drainage layer exists within the layer, the drainage path becomes long. In such a case, forming the drainage layer by installing sand drains shortens the drainage length, discharges the water faster, and accelerates the consolidation.

2) Paper Drain (Cylindrical Drain) Method

In the paper drain method, cardboard that dewaters well is driven into the cohesive ground to drain the pore water out to the ground surface and accelerates the consolidation settlement.

3) Pack Drain Method

The pack drain method improves the shortcoming of the sand drain method, which is prone to drain sections becoming discontinuous. A polyethylene mesh pack is filled with sand to form a column, which is driven into the ground to accelerate the consolidation drainage. Unlike sand drains, pack drains are not placed in equal spacing due to the characteristics of the equipment. The average degree of consolidation is calculated based on the tributary area of each drain, as shown in Figure 2.4.4.

In case the drains are placed in a rectangular pattern, the diameter of the equivalent influence circle is defined as,

$$d_{e1} = 1.128 \cdot L_1 \quad ; \quad d_{e2} = 1.128\sqrt{L_1 \cdot L_2} \quad ; \quad d_{e3} = 1.128 \cdot L_2 \qquad (2.4.23)$$

The time factor, T_h is given by,

$$T_{h1} = \frac{C_h \cdot t}{d_{e1}^2} \quad ; \quad T_{h2} = \frac{C_h \cdot t}{d_{e2}^2} \quad ; \quad T_{h3} = \frac{C_h \cdot t}{d_{e3}^2} \qquad (2.4.24)$$

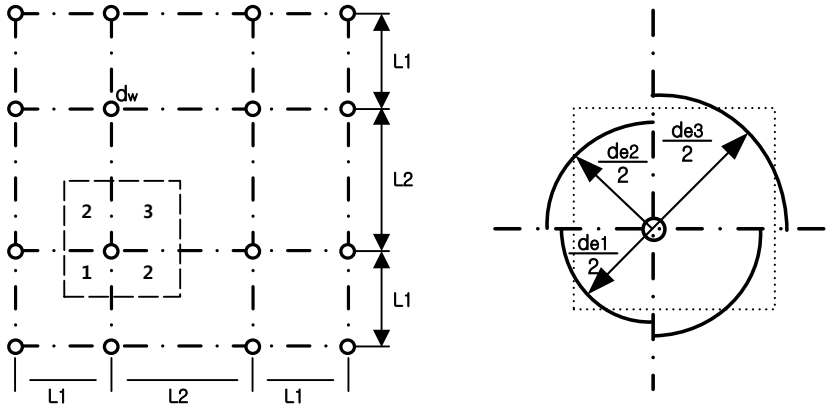

Figure 2.4.4 Spacing of pack drains

The spacing ratio (n) of each divided zone is as follows:

$$n_1 = \frac{d_{e1}}{d_w} \quad ; \quad n_2 = \frac{d_{e2}}{d_w} \quad ; \quad n_3 = \frac{d_{e3}}{d_w} \tag{2.4.25}$$

The average degree of consolidation from the above is calculated as,

$$U = \frac{A_1U_1 + 2A_2U_2 + A_3U_3}{A_1 + 2A_2 + A_3} \tag{2.4.26}$$

4) Sand Compaction Pile or Gravel Compaction Pile Method

The sand compaction pile method pressure-inserts sand or gravel into the soft ground by applying vibratory loads to form compacted piles. This method increases the density of soil, which in turn induces an increase in bearing capacity, a decrease in consolidation settlement, and an increase in lateral resistance, and promotes homogeneous ground and the effect of consolidation drainage. The method can be used in almost every soil types such as loose sandy soil, cohesive soil, organic soil, etc.

The ratio of substitution (a_s) represents the degree of improvement, which is expressed in the ratio of the volume of sand (gravel) pile to the volume of the original ground being set to 1. In general, the substitution ratio is less than 0.3 for improvement of sandy soil or in-land cohesive soil and 0.3-0.8 for the ground underwater.

Placement in a rectangular pattern (b): $a_s = \frac{A_s}{A} = \frac{A_s}{d^2}$

Placement in a square pattern (c): $a_s = \frac{A_s}{A} = \frac{2}{\sqrt{3}} \cdot \frac{A_s}{d^2}$

where,

A_s : Cross sectional area of sand (gravel) pile

A : Cross sectional area of sand (gravel) pile
+ cross sectional area of cohesive soil

When structures are loaded on the foundations of complex ground, which is composed of cohesive soil and sand (gravel) piles, the cohesive soil and the sand (gravel) piles experience different stress distributions and magnitudes. In general, the stress becomes concentrated on the sand (gravel) piles due to the difference in physical and mechanical properties between the cohesive soil and the compressed sand (gravel) piles.

In case of sandy soil, it is unclear as to the increase in the strength of the initial ground due to compaction. For cohesive soil, the theory well explains the effect of complex ground, which is composed of cohesive soil and sand piles. Because of the concentration of stresses on the sand piles, the significant reduction in stresses in the cohesive soil results in an increase in the bearing capacity of the complex foundations and a decrease in settlement.

As shown in Figure 2.4.5, an average stress, σ applied to the complex ground results in ground reactions; σ_s occurs in the piles and σ_c occurs in the cohesive soil. The following equation is obtained assuming that the stress is constant within each area, A_s and A_c:

$$\sigma \cdot A = \sigma_s \cdot A_s + \sigma_c \cdot A_c \qquad (2.4.27)$$

Transforming the equation using the stress distribution ratio $\left(n = \sigma_s / \sigma_c\right)$ gives,

$$\sigma \cdot A = n \cdot \sigma_c \cdot A_s + \sigma_c \cdot A_c = \sigma_c \left(n \cdot A_s + A_c\right) \tag{2.4.28}$$

The stress ratios of the piles and the cohesive soil are given by,

$$\mu_s = \frac{\sigma_s}{\sigma} = \frac{n \cdot A}{n \cdot A_s + A_c} = \frac{n}{1 + (n-1) a_s} \tag{2.4.29}$$

$$\mu_c = \frac{\sigma_c}{\sigma} = \frac{A}{n \cdot A_s + A_c} = \frac{1}{1 + (n-1) a_s} \tag{2.4.30}$$

where,

μ_s : Stress concentration factor for piles

μ_c : Stress reduction factor for cohesive soil

a_s : Substitution ratio of sand (gravel) $\left(a_s = A_s / A\right)$

The following relationship is obtained from the above equation:

$$\mu_s \cdot a_s + \mu_c \left(1 - a_s\right) = 1 \tag{2.4.31}$$

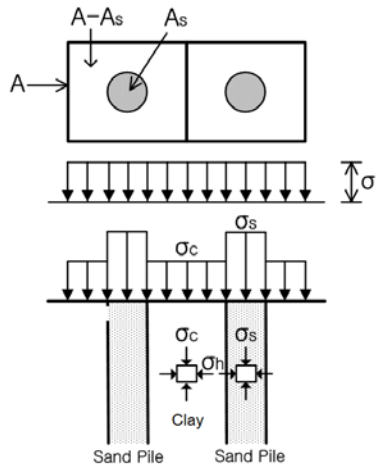

Figure 2.4.5 Stress distribution of sand compaction piles

The general stress distribution ratios (n) used in practice are dependent on the substitution ratios (a_s) as shown in Table 2.4.3. When n is obtained by measuring the in-situ stress of the soil, μ_s and μ_c can be calculated from the above equations.

Table 2.4.3 Stress distribution ratio (n)

Substitution ratio (a_s)	Internal friction angle of sand (gravel) (ϕ_s)	Stress distribution ratio (n)
0 - 0.4	30	3
0.4 - 0.7	30	2
Above 0.7	30 - 35	1

The diameter of an equivalent influence circle in general vertical drain methods is calculated as shown in Figure 2.4.6.

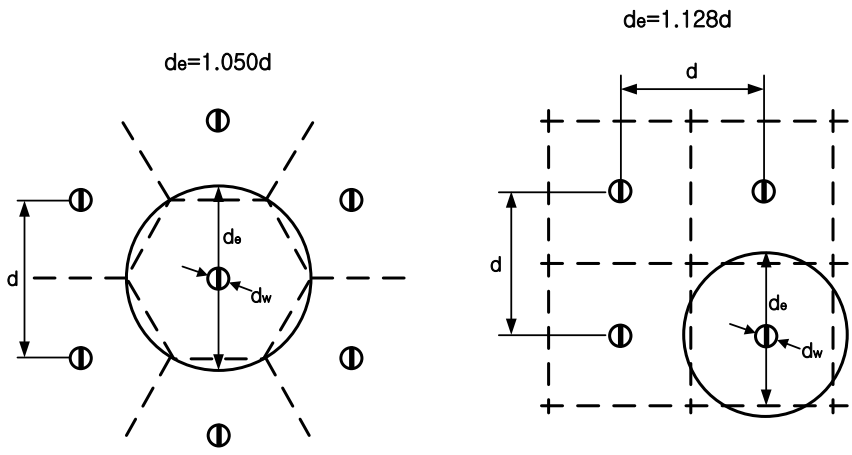

(a) Placement in a triangular pattern

(b) Placement in a square pattern

Figure 2.4.6 Diameters of equivalent influence circles

2.4.3.4 Calculation of Consolidation for Complex Ground

The calculation of consolidation in complex ground is not too different from that for sand drains, but the design method is different. The settlement is measured on site, and the magnitude of settlement can be also empirically estimated. In general, the settlement of complex ground is between 1/3 and 2/3 of the settlement of unimproved ground. This can be viewed as due to the effect of the ground improvement and the characteristics of complex ground. The settlement of complex ground is determined by the vertical stress in the cohesive soil.

The degree of consolidation is calculated, generally assuming that the sand compacted piles act as the vertical drainage piles. The settlement of complex ground is characterized by the decrease in settlement, and this is because the stress in cohesive soil is smaller than that in the sand piles. The larger the magnitude of the substitution ratio (a_s), the smaller is the settlement.

This chapter describes the method of calculating the settlement of complex ground using the equilibrium method presented by Aboshi et al. (1979) and Barksdae et al. (1981). The assumptions used in this method are as follows:

The concept of unit cell (equivalent effective circumference) is applied to the entire ground.
The overburden pressure applied to the unit cell equals the sum of the stresses in cohesive soil and sand piles (equilibrium is maintained).
The settlements of sand piles and cohesive soil are the same.
The stress induced by the overburden pressure in a sand pile is constant over the total length of the pile or within an element when a compressible layer is divided into a number of elements.

The final consolidation settlement by the C_c method is expressed as,

$$S_f = \frac{C_c}{1+e_0} \cdot H \cdot \log_{10}\left(\frac{\sigma_0 + \mu_c \sigma}{\sigma_0}\right) \qquad (2.4.32)$$

The ratio of the settlement of complex ground to that of unimproved ground is given by,

$$\beta = \frac{S_f}{S} = \frac{\log_{10}\left(\frac{\sigma_0 + \mu_c \sigma}{\sigma_0}\right)}{\log_{10}\left(\frac{\sigma_0 + \sigma}{\sigma_0}\right)} \tag{2.4.33}$$

where,

σ_0 : Initial effective overburden pressure

σ : Overburden pressure due to loading.

If the effective stress, σ_0 is very large (when the sand pile is long) and the overburden pressure, σ is small, $\beta = \frac{S_f}{S}$ ratio converges to μ_c.

$$\beta = \frac{S_f}{S} \approx \mu_c = \frac{1}{1 + (n-1)a_s} \tag{2.4.34}$$

2.5 Increase in Ground Strength due to Embankment Load

2.5.1 General Equation

The strength increase ratio (m) for cohesive soil due to embankment is expressed as the ratio of the undrained strength in the natural condition, C_u to the applied overburden pressure, P_0. The strength increase due to the loading is given by,

$$C = C_0 + m\left(P_0 + \Delta P - P_c\right)U \tag{2.5.1}$$

where,

C	: Cohesion
C_0	: Initial cohesion
ΔP	: Load increment
m	: Strength increase ratio
U	: Degree of consolidation
P_0	: Effective overburden pressure
P_c	: Preconsolidation load

2.5.2 Strength Increase due to SCP or GCP Process

When ground is improved by the sand compaction pile method or gravel compaction pile method, the strength increase is calculated as follows:

$$\phi = \tan^{-1}\left(m \cdot \tan\phi_s\right) \tag{2.5.2}$$

$$C = \left(1 - a_s\right)\left[C_0 + m\left(P_0 - P_c + \mu_c \cdot \sigma\right)U\right] \tag{2.5.3}$$

where,

m	: Strength increase ratio
ϕ_s	: Internal friction angle of sand (gravel)

μ_s : Stress increase factor of pile $\left(\mu_s = \frac{\sigma_s}{\sigma} = \frac{n}{1+(n-1)a_s}\right)$

μ_c : Stress reduction factor of cohesive soil $\left(\mu_c = \frac{\sigma_c}{\sigma} = \frac{1}{1+(n-1)a_s}\right)$

σ_s : Stress distributed in sand (gravel)

σ_c : Stress distributed in cohesive soil

σ : Stress increase due to embankment loads

a_s : Substitution ratio (A_s/A)

n : Stress distribution ratio

2.6 Settlement over Time under Staged Loading

2.6.1 Introduction

Embankment loads or external loads applied to improve soft ground are loaded by stages considering the loading period and the loading placement period. Loading at the next stage is applied before the consolidation due to the embankment load at the previous stage is completed. The settlement curve after two stages of loading becomes complex because the settlements due to the first loading and the second loading coexist.

In the reality of a construction site, the total load is gradually loaded rather than applying the total load instantaneously. If the period of placing an embankment or a structure is relatively very short compared to the consolidation time, the load can be considered to have been instantaneously loaded as an approximation. On the contrary, if the consolidation during the application of loads is significant, the consolidation should be calculated on the basis of incremental loading.

SoilWorks supports both the total load method and the incremental load method to calculate the time-settlement relationship by stages.

2.6.2 Total Load Method

The total load method calculates the settlements over time and the total settlement for the total accumulated load at each stage of loading, when embankment loads or external loads are applied by stages. The ground condition at each stage is defined by the initial original ground condition. That is, the settlements over time are calculated for the initial ground condition at the first stage of loading, and the settlements over time are calculated for the initial ground condition at the second stage of loading. The second stage settlement curve is then horizontally shifted back to intersect with the first stage curve at the time of the second stage loading.

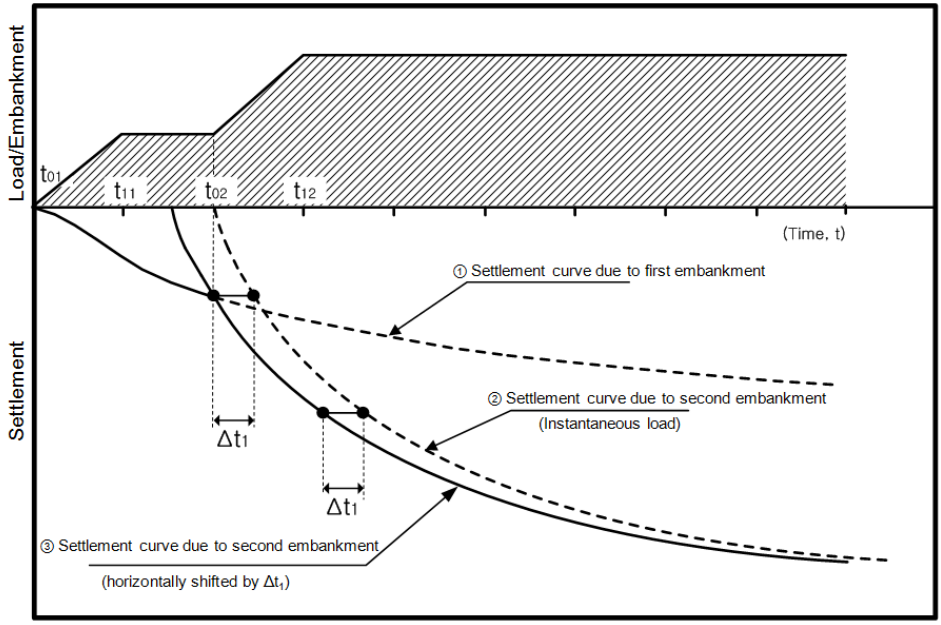

Figure 2.6.1 Horizontal shift of settlement curve under staged embankments

2.6.2.1 Settlement Curve at Loading Stage

1) Settlement Curve for Undrained Soil

$t_{0m} < t < t_{1m}$ (Loading period)

For undrained soil, the time factor, T_{vt} of the loading period is given by,

$$T_{vt} = \frac{C_v \left[\frac{(t - t_{0m})}{2} + \Delta t_1 \right]}{H_0^2} \tag{2.6.1}$$

where,

C_v : Coefficient of consolidation

H_0 : Thickness of consolidation layer of the original ground

t : Time (day)

t_{0m} : Start day of loading the m th stage embankment

Δt_1 : Time of horizontal shift

The degree of consolidation, U_m at the m th stage embankment is expressed as,

$$U_m = \sqrt{\frac{4T_{vt}}{\pi}} \quad \text{for} \quad U_m \le 53\% \tag{2.6.2}$$

$$U_m = 1 - \frac{10^{\frac{1.781 - T_{vt}}{0.933}}}{100} \quad \text{for} \quad U_m > 53\% \tag{2.6.3}$$

The horizontally shifted time, Δt_1 at the m th stage embankment is given by,

$$\Delta t_1 = \frac{H_0^2 \pi U^2}{4C_v} \quad \text{for} \quad U \le 53\% \tag{2.6.4}$$

$$\Delta t_1 = \frac{H_0^2 \left[1.781 - 0.933 \times \log(100 - 100U)\right]}{C_v} \quad \text{for} \quad U > 53\% \tag{2.6.5}$$

where,

$U = S_{(t0m)(m-1)} / S_f$

$S_{(t0m)(m-1)}$: Settlement at the start day of the m th stage embankment due to the loading upto the $m-1$ th stage

S_f : Final settlement when loading the m th stage load

The consolidation settlement, S_{tm} during the loading period at the m th stage embankment is defined as,

$$S_{tm} = \left(S_f U_m - S_{(t0m)(m-1)}\right)\left(\frac{t - t_{0m}}{t_{1m} - t_{0m}}\right) + S_{(t0m)(m-1)} \tag{2.6.6}$$

where,

t_{0m} : Start day of loading at the m th stage embankment

t_{1m} : End day of loading at the m th stage embankment

$t_{1m} < t$ (Placement period)

The time factor, T_{vt} is expressed as,

$$T_{vt} = \frac{C_v \left[t - \frac{(t_{0m} + t_{1m})}{2} + \Delta t_1 \right]}{H_0^2} \tag{2.6.7}$$

The degree of consolidation, U_m is expressed in Eq. (2.6.2) and (2.6.3). The horizontally shifted time, Δt_1 is expressed in Eq. (2.6.4) and (2.6.5). The consolidation settlement, S_{tm} during the placement time at the time of the m th stage embankment is given by,

$$S_{tm} = S_f U_m \tag{2.6.8}$$

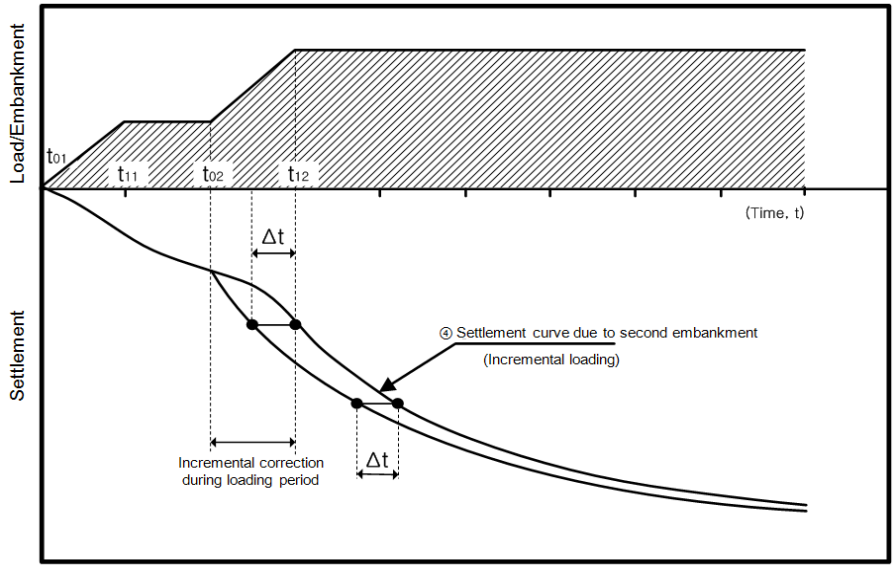

Figure 2.6.2 Incremental correction of settlement curve under staged embankment construction

As shown in Figure 2.6.1, when embankment is incrementally constructed in two stages, the settlement curve ② due to the instantaneous loading condition from the second stage is horizontally shifted by Δt_1 to intersect with the settlement curve from the first stage at t_{02}. The curve ③ represents the horizontally shifted curve. Subsequently, the settlement curve ④ is drawn by performing incremental correction during the loading period of the second stage as shown in Figure 2.6.2. At this point, a horizontal shift by Δt takes places together with the incremental correction. Δt is determined by iteration.

2) Settlement Curve for Drained Soil

$t_{0m} < t < t_{1m}$ (Loading period)

For drained soil, the time factor, T_{ht} of the loading period is given by,

$$T_{ht} = \frac{C_h\left[\frac{(t-t_{0m})}{2} + \Delta t_1\right]}{d_e^2} \tag{2.6.9}$$

where,

C_h : Coefficient of consolidation in the horizontal direction

d_e : Diameter of influence circle

The degree of consolidation, U_m can be determined by a number of different methods (refer to Section 2.4.3).

$$U = 1 - \exp\left(\frac{-8T_h}{F(n)}\right) \quad \text{: Barron method} \tag{2.6.10}$$

$$U = 1 - \exp\left(\frac{-8T_h}{F}\right) \quad \text{: Hansbo method} \tag{2.6.11}$$

$$U = 1 - \exp\left(\frac{-8T_h}{m}\right) \quad \text{: Yoshikuni method} \tag{2.6.12}$$

$$U = 1 - \exp\left(\frac{-8T_h}{F(n') + 0.8L}\right) \quad \text{: Onoue method} \tag{2.6.13}$$

The horizontally shifted time, Δt_1 at the m th stage embankment is expressed as,

$$\Delta t_1 = \frac{d_e^2 \pi U^2}{4 C_h} \quad \text{for} \quad U \le 53\% \tag{2.6.14}$$

$$\Delta t_1 = \frac{d_e^2 \left[1.781 - 0.933 \times \log(100 - 100U)\right]}{C_h} \quad \text{for} \quad U > 53\% \tag{2.6.15}$$

where,

$U = S_{(t0m)(m-1)} / S_f$

$S_{(t0m)(m-1)}$: Settlement at the start day of the m th stage embankment
Due to the loading upto the $m-1$ th stage

S_f : Final settlement when loading the m th stage load

The consolidation settlement, S_{tm} during the loading period at the m th stage embankment is expressed in Eq. (2.6.6).

$t_{1m} < t$ (Placement period)

The time factor, T_{ht} is expressed as,

$$T_{ht} = \frac{C_h \left[t - \frac{(t_{0m} + t_{1m})}{2} + \Delta t_1 \right]}{d_e^2} \tag{2.6.16}$$

The consolidation settlement, S_{tm} during the placement period at the m th stage embankment is defined in Eq. (2.6.8).

2.6.2.2 Settlement Curve at Unloading Stage

When an embankment or external load is removed during embankment, a rebound occurs in cohesive soil, the calculation for which is described in Section 2.2.3. As shown in Figure 2.6.3, the stages 1, 2 and 4 are subjected to loading, and the stage 3 is subjected to unloading. Now the settlement curve is prepared for embankment construction in four stages. If the settlement (Point A) at the time t_{03} reflecting the rebound at the unloading stage 3 is less than the final settlement from the stage 1, the horizontal shift of Δt takes place as shown in Figure 2.6.3, which is the reduced settlement time at the stage 1.

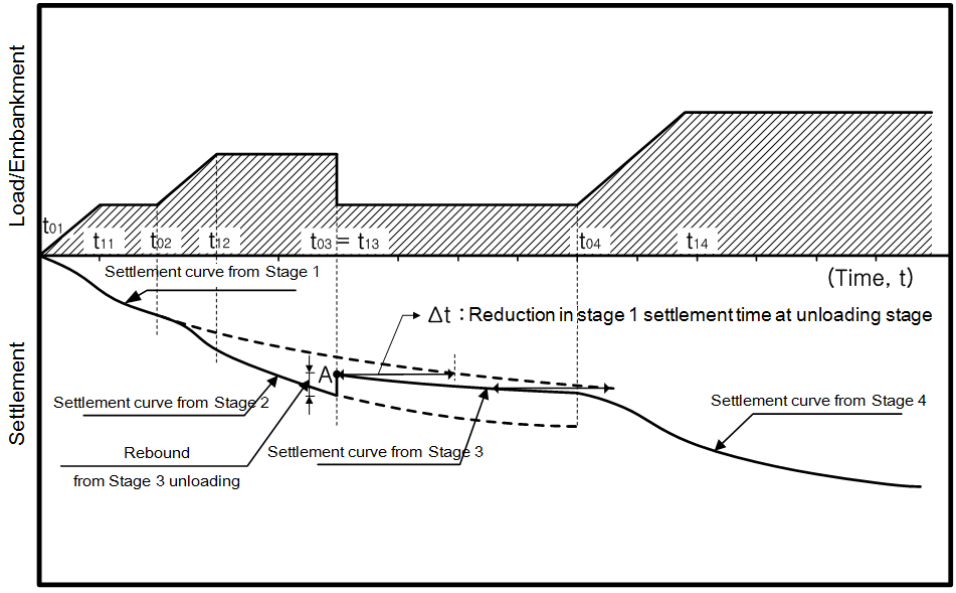

Figure 2.6.3 Horizontal shift of settlement curve at unloading stage

If the point A is greater than the final settlement from the stage 1, the settlement at the point A can be constantly maintained until the start point of the subsequent stage as shown in Figure 2.6.4.

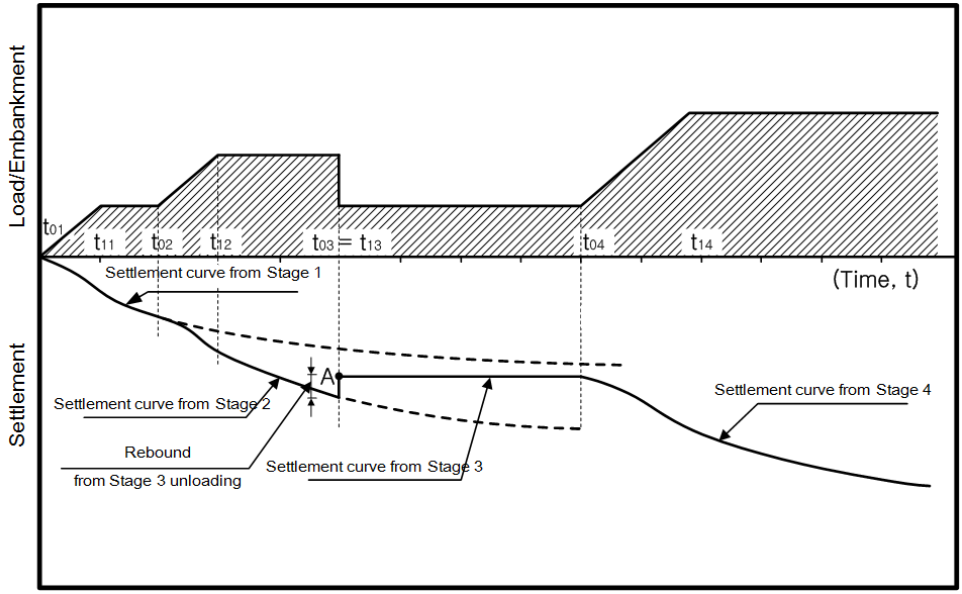

Figure 2.6.4 Constant settlement at unloading stage

2.6.3 Individual Load Method

When embankment loads or external loads are loaded by stages, the individual load method calculates the settlements over time and the total settlement for the net load pertaining to each stage, which are then accumulated to determine the overall settlement curve. The ground condition at each stage changes with time. That is, the settlements over time are calculated for the stage 1 loading based on the initial ground condition. From the stage 2 loading, the settlement layer is recomposed to reflect the change in effective stress and the settlement taken place in the ground. The final settlement curve is obtained by accumulating the settlement curves of the individual stages.

Figure 2.6.5 illustrates the way of accumulating the settlement curves from the stages 1 and 2.

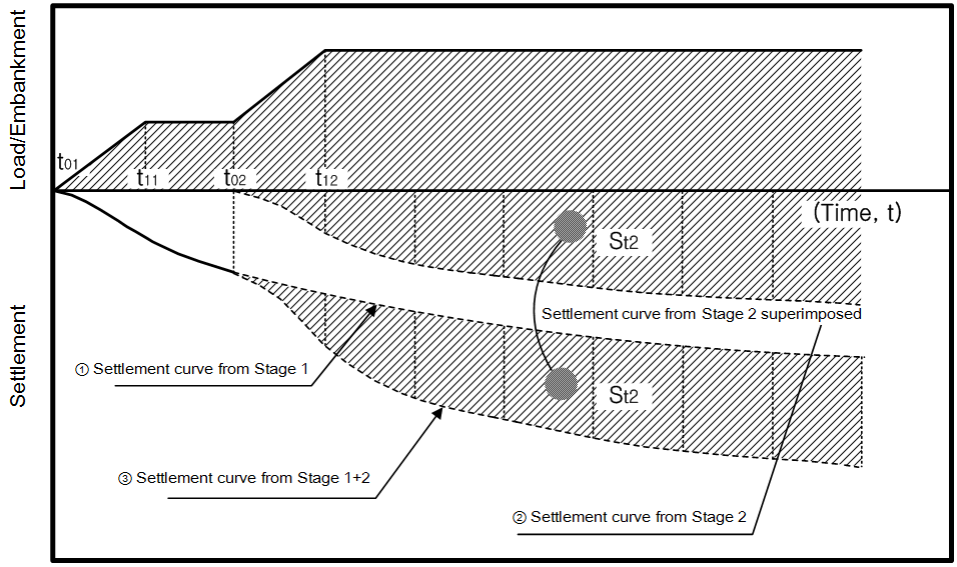

Figure 2.6.5 Accumulation of settlement curves by individual load method

Figure 2.6.6 shows the first 3 stages of embankment followed by unloading at the stage 4. The settlement curves for the stages 1, 2 and 3 are accumulated, and the rebound at the start day of the stage 4 unloading is deducted with the constant settlement maintained at a horizontal curve. The settlement curve at the stage 4 then becomes the accumulated settlement curves 1+2+3+4.

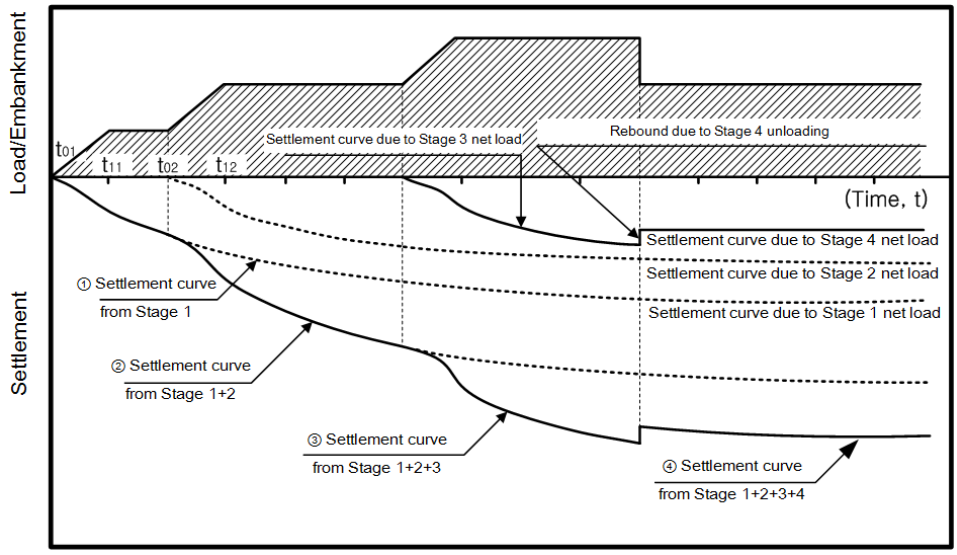

Figure 2.6.6 Accumulation of settlement curves under unloading by individual load method